

# **KERNFORSCHUNGSZENTRUM KARLSRUHE**

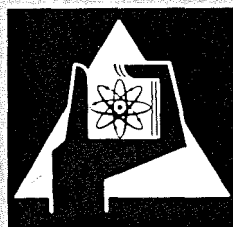
Oktober 1972

KFK 1675

Institut für Angewandte Kernphysik

**The Karlsruhe Fast Neutron Time-of-Flight Facility**

S. Cierjacks



**GESELLSCHAFT FÜR KERNFORSCHUNG M. B. H.  
KARLSRUHE**

Als Manuskript vervielfältigt

Für diesen Bericht behalten wir uns alle Rechte vor

GESELLSCHAFT FÜR KERNFORSCHUNG M. B. H.  
KARLSRUHE

KERNFORSCHUNGSZENTRUM KARLSRUHE

August 1972

KFK 1675

Institut für Angewandte Kernphysik

The Karlsruhe Fast Neutron Time-of-Flight Facility

S. Cierjacks

Gesellschaft für Kernforschung m.b.H., Karlsruhe

Invited Paper

International Conference on Nuclear Structure Study with  
Neutrons, Budapest, Hungary, July 31 - August 5, 1972.



## ABSTRACT

The fast neutron time-of-flight spectrometer installed at the Karlsruhe sector-focussed cyclotron is discussed as an example of a high intensity pulsed neutron source. A description of the operation principles of this facility, a few examples of typical measurements which have been carried out and an outline of the scope and the capability of the spectrometer is given. The performance data for this spectrometer are compared with those for some other accelerator-based high intensity neutron sources in Europe.

## ZUSAMMENFASSUNG

Das hochauflösende Neutronenflugzeitspektrometer am Karlsruher Isochron Zyklotron wird als ein Beispiel für eine sehr intensive Neutronenquelle diskutiert. Das Prinzip der internen Strahlenablenkung zur Untersetzung der Pulsfolgefrequenz unter weitgehender Erhaltung der mittleren Strahlintensität wird beschrieben. Anhand einiger Beispiele für typische Experimente, die bisher mit dem Spektrometer ausgeführt wurden, wird die Leistungsfähigkeit der Anlage demonstriert. Die Spezifikationen des Karlsruher Flugzeitspektrometers werden mit denen ähnlicher Einrichtungen an verschiedenen anderen Beschleunigern verglichen.



# THE KARLSRUHE FAST NEUTRON TIME-OF-FLIGHT FACILITY

S. Cierjacks

Institut für Angewandte Kernphysik  
Kernforschungszentrum Karlsruhe, Karlsruhe  
F.R. Germany

Abstract: The fast neutron time-of-flight spectrometer installed at the Karlsruhe sector-focussed cyclotron is discussed as an example of a high intensity pulsed neutron source. A description of the operation principles of this facility, a few examples of typical measurements which have been carried out and an outline of the scope and the capability of the spectrometer is given. The performance data for this spectrometer are compared with those for some other accelerator-based high intensity neutron sources in Europe.

## I. Introduction

Although the area of resonance neutron spectroscopy is presently dominated by pulsed neutron sources based on electron linacs, the highest instantaneous neutron intensities are provided by acceleration of positive charged particles to high energies. While advanced types of circular and linear accelerators hold great promise for the future, this concept has not in general been realized because of technological problems such as heat transfer etc.. Certain existing machines do, however, permit us to partially realize this concept already at present. A high energy proton linear accelerator to be used as a high intensity neutron source will be described by Dr. Moore in an other invited talk of this conference. Of the circular accelerators the sector-focussed cyclotron is currently best able to take advantage of this capability. This machine combines both, high beam intensity and narrow pulse width of a few nanoseconds. For proper use of this machine additional equipment is necessary because sector-focussed cyclotrons run continuously with a microstructure pulse recurrence frequency of 10-30 MHz which is far too high in view of frame overlap problems. It is obvious that for long flight paths the time interval of 30-100 nsec between two subsequent pulses is so short that slow neutrons from a preceding pulse can be overtaken by fast neutrons from the following pulse. A reduction of the recurrence frequency by suppression of most of the microstructure pulses

would entail a tremendous sacrifice in intensity. Therefore, it is desirable to reduce the recurrence frequency while largely preserving the high average beam intensity of a sector-focussed cyclotron. This condition has been met with a new 'deflection-bunching' system, which was developed for use with the Karlsruhe 50 MeV machine. With this particular system the repetition rate for neutron production can be reduced from 33 MHz to 200 kHz while the average beam intensity is decreased only by a factor of 3<sup>1,2)</sup>.

In this talk I will give a description of the operation principles of the Karlsruhe fast neutron facility, a few examples of typical measurements we have carried out and an outline of the scope and capabilities of the spectrometer. Finally the Karlsruhe neutron time-of-flight spectrometer will be compared with some other high intensity neutron sources in Europe.

## II. The Karlsruhe Fast Neutron Facility

### A. Principle of Operation

The reduction of the pulse repetition rate in the Karlsruhe sector-focussed cyclotron is accomplished by two coupled electrostatic deflector assemblies which together form the 'deflection bunching' system. A scheme of the 'deflection bunching' system is shown in fig. 1.

In normal continuous operation of the Karlsruhe cyclotron three microstructure pulses are delivered from the source since acceleration is accomplished in the third harmonic mode. This gives rise to an instantaneous beam distribution which is indicated by the three regions between the dotted lines. The deflector system which is located near the center of the machine (deflector I) is used for a twofold purpose:

- i) to eliminate two out of three microstructure pulses by deflection to a beam stop and
- ii) to form ion packets of 4,5  $\mu$ sec duration (each consisting of 50 microstructure pulses) with a repetition rate up to 200 kHz.

As a result of this kind of deflection only the portion of the beam indicated by hatching will remain.

Both these objectives have been achieved with a suitable combination of a radial and an axial electrostatic deflector provided with an appropriate sinusoidal deflection voltage superimposed on a square



wave high voltage pulse. This is illustrated in fig. 2. The upper curve shows the normal pulse structure at the position of the inner deflector plates (deflector I). If a deflection voltage of the form shown in the next lower curve is supplied to a radial deflector only every third microstructure pulse will pass this system because the voltage then is decreased to zero. The formation of the ion packet is explained in the lower two curves of fig. 2. The bottom curve shows the deflection voltage which is supplied to an additional axial deflector. Since the deflection voltage decreases to the zero level for 4.5  $\mu$ sec only once during the pulse recurrence cycle, an ion packet as shown in the curve above is formed.

The subsequent procedure with the remaining beam is analogous to the treatment of beam deflection for neutron time-of-flight experiments in synchrocyclotrons: A second axial deflector (deflector II of fig. 1) is located at the maximum radius of the machine with the plates above and below the medium plane of the cyclotron. This deflector serves to simultaneously deflect the whole set of microstructure pulses to a neutron producing target positioned above the medium plane of the cyclotron (see fig. 1b). At the time of deflection, the entire packet which is distributed over 10 cm in radius must be completely inside the area covered by the deflection plates. Before striking the target the deflected beam completes almost an additional revolution.

It is evident from this description that such a procedure produces single neutron pulses of the same pulse duration as the microstructure pulses, that is  $\sim 1$  nsec, but increases the intensity in the neutron burst by almost a factor of 50.

#### B. Performance of the Neutron Spectrometer

A top view of the spectrometer arrangement is shown in fig. 3. For neutron production a thick natural uranium target is used. Collimators are positioned in the flight path to define a narrow neutron beam with a solid angle of  $\sim 2 \cdot 10^{-6}$  sr. The neutrons are detected at the end of an evacuated flight path the present length of which is 195 m. A typical unmoderated time-of-flight spectrum is shown in fig. 4. The broad pronounced maximum peaked near 18 MeV is due to neutrons from deuteron break-up processes. The flat distribution at energies below  $\sim 6$  MeV originates mainly from evaporation

and fission processes. It is apparent from this illustration that the useful energy range for measurements with unmoderated spectra is between several hundred keV and  $\sim 30$  MeV. The performance data of our neutron spectrometer are summarized in table I.

### III. Examples of Typical Measurements

Since its completion in 1966 the fast neutron time-of-flight spectrometer has been extensively used for high resolution neutron experiments.

In the beginning a series of high resolution transmission experiments were carried out for a few separated isotopes and a large number of elements <sup>3)</sup>. The early investigations with the 60 m flight path were complemented by very high resolution measurements employing the new 195 m flight path <sup>4)</sup>. At a later stage high resolution measurements of elastic and inelastic neutron scattering processes were performed <sup>5)</sup>. In the last three years the spectrometer has also been used for the study of neutron induced fission processes <sup>6)</sup> and the investigation of (n,x)-reactions <sup>7)</sup>.

The objective of our program of high resolution neutron experiments apart from the accurate determination of the cross sections is the systematic study of fast neutron reactions and of nuclear structure phenomena. The average energy dependence of neutron total and partial elastic and inelastic scattering cross sections over the wide energy region of 30 MeV allows to study the range of validity of optical model and Hauser-Feshbach calculations. Resonance parameter determination of individual resonances in light and medium weight nuclei up to several MeV can extend our present knowledge on level statistics considerably. From this information accurate strength functions of not only s- but also higher partial waves can be deduced. Fluctuation analysis of the structure observed in total and partial neutron cross sections in the region of overlapping compound-nucleus resonances provides a good means to determine average level densities and level widths and thus, to check the validity of statistical assumptions. Total and differential cross sections for the scattering of neutrons on light nuclei near closed shells can be used for comparison with the predictions of microscopic theories of nuclear reactions. The predictions for simple one particle - one hole states which can be treated by coupled channel equations in the continuum shell-model are currently of particular interest. Excitation functions of (n,x)-reactions along with

the energy and angular distributions of the emitted charged particles provide a good means for the study of excited states in the residual nuclei and of reaction mechanisms.

A few experimental results which have been obtained with the Karlsruhe time-of-flight facility might demonstrate the capability of the spectrometer. In fig. 5 the highly resolved total cross section of oxygen between 3-7 MeV is shown. For this light nucleus individual resonances are still apparent up to excitation energies of more than 10 MeV. The resolution of our spectrometer allowed us to observe a number of narrow resonances which either have not been seen or not been fully resolved in earlier neutron experiments. A high resolution elastic neutron scattering measurement is shown in fig. 6. The differential elastic scattering cross section of calcium is plotted as a function of energy separately for three different scattering angles. Such data have provided a good means to identify spins and parities of closely spaced resonances from a study of the resonance shapes as a function of scattering angle <sup>8)</sup>. Fig. 7 demonstrates the capability of the spectrometer in the field of inelastic neutron scattering. These curves show the energy dependent cross section for the production of the 843 keV  $\gamma$ -line by inelastic neutron scattering in iron. With the resolution obtained for these measurements it was possible to study the complicated structure of nuclei such as iron separately for different inelastic channels <sup>9)</sup>.

#### IV. Comparison With Other Accelerators

The most important European accelerators which are extensively used as pulsed neutron sources are listed in table II. Included for comparison is also ORELA, the Oak Ridge electron linac. With the exception of a second set of performance data for the Geel linac which represent a proposed improvement <sup>10)</sup> of the machine (operation with four sections and new gun), the data for all other installations reflect present operation conditions. The most important specifications of these installations are contained in columns 6-8 and 10. These are the pulse duration, the maximum repetition rate, the neutron production in the pulses and the energy resolution. The latter quantity is quoted in terms of the best nominal value, i.e. the value for the shortest machine pulse length and the longest flight path. For the existing installations the highest instantaneous neutron intensities are

obtained with the cyclotrons. Of these the Harwell synchrocyclotron has the highest value. The highest resolution is obtained for the Karlsruhe sector-focussed cyclotron. But also ORELA and the Geel linac have very good energy resolution when operated in the short-pulse, long flight path mode.

Although useful for comparison of identical quantities, table II cannot be directly used to judge the overall character of pulsed accelerator installations. In order to compare different accelerators as pulsed neutron sources in an adequate way, one has to establish some more general criteria. In the past a number of authors have proposed criteria for comparison of different types of accelerators used for neutron production<sup>11-14)</sup>.

To my mind the best approach is that suggested by Rae<sup>15)</sup> in his extensive and detailed recent review. As a measure of the quality of a pulsed neutron facility he adopted for a given effective energy resolution the useful flux available at the detector. In estimating the neutron flux in a fixed energy interval  $\Delta E$  of effective resolution  $\Delta E/E$  not only the neutron intensity during the pulse but also the geometry and efficiency of the moderator and the limitation in intensity imposed by the use of overlap filters at high repetition rates and low energies were taken into account.

A comparison employing this criterion for a number of accelerators is shown in fig. 8 which was taken from Rae's work. Here the neutron flux available for the several current accelerators at the detector is plotted as a function of energy and for an effective energy resolution of  $\Delta E/E = 8.8 \cdot 10^{-4}$ . The diagram shows the Harwell booster, the Oak Ridge linac, the Harwell synchrocyclotron and the Karlsruhe sector focussed cyclotron. The numbers in the brackets behind the symbols are the machine pulse lengths in nsec. The values near each curve are the pulse repetition frequencies and the lengths of flight path needed to preserve the constant value of  $\Delta E/E$ . Flight path length up to 300 m have been assumed where necessary, irregardless of whether the paths actually exists or not. This flexibility is reasonable, since presently existing flight paths are not necessarily due to the optimum capabilities of the accelerators. It is apparent from this illustration that the Karlsruhe cyclotron with its very short pulse length has the highest neutron flux and is dominant in the fast neutron region. However, it would not be very useful to employ

the Karlsruhe machine at energies below a few hundred keV because the high neutron intensity can only be preserved for high repetition rates. The Harwell synchrocyclotron gives the best performance between a few hundred and about 10 keV, while ORELA with 16 and 2.5 nsec pulse operation has the most flexible performance for use over a wide energy range and is superior to the other machines between  $\sim 100$  eV and 10 keV. The Harwell booster has the best specifications in the range below 100 eV.

The principle conclusion I would like to draw from this discussion is that each machine has its own merits which can be exploited by careful selection of experiments. With respect to our own machine I would like to stress that the Karlsruhe sector-focussed cyclotron has proven to be a very powerful device for fast neutron experiments in the previously poorly explored energy region above several hundred keV.

References

1. S. Cierjacks, P. Forti, L. Kropp, H. Unseld, Proc. Sem. Intense Neutron Sources, Santa Fe<sup>1</sup>, September 1966, USAEC CONF-660925 , p. 589
2. S. Cierjacks, B. Duelli, P. Forti, D. Kopsch, L. Kropp, M. Lösel, J. Nebe, H. Schweickert, H. Unseld, Rev. Sci. Instr. 39 (1968) 1279
3. S. Cierjacks, P. Forti, D. Kopsch, L. Kropp, J. Nebe, H. Unseld, Kernforschungszentrum Karlsruhe Report, KFK-1000, June 1968; B. Zeitnitz, H. Dubenkropp, R. Putzki, G.J. Kirouac, S. Cierjacks, J. Nebe, C.B. Dover, Nucl. Phys. A 160 (1971) 443; S. Cierjacks, P. Forti, G.J. Kirouac, D. Kopsch, L. Kropp, J. Nebe, Phys. Rev. Letters 23 (1969) 866 C
4. S. Cierjacks, Proc. Int. Conf. Nuclear Data for Reactors , Vol II, p 219, Helsinki, June 1970; and D. Kopsch, S. Cierjacks, G.J. Kirouac, ibid p. 39
5. J. Nebe, G.J. Kirouac, Nucl. Phys. A 185 (1972) 113; and G.J. Kirouac, J. Nebe, Nucl. Phys. A 154 (1970) 36; F. Voß, S. Cierjacks, L. Kropp, Proc. Conf. Neutron Cross Sections and Technology, Knoxville, March 1971, CONF-710301, Vol I, p.219
6. S. Cierjacks, D. Kopsch, J. Nebe, G. Schmalz, F. Voß, Proc. Conf. Neutron Cross Sections and Technology, Knoxville, March 1971, CONF-710301, Vol II, p.280
7. L. Kropp, Kernforschungszentrum Karlsruhe Report, KFK-1190 (1970); and L. Kropp, P. Forti, Nucl. Instr. Methods (to be published)
8. J. Nebe, G.J. Kirouac, Kernforschungszentrum Karlsruhe Report KFK-1189 (1970); and G.J. Kirouac, J. Nebe, Kernforschungszentrum Karlsruhe Report, KFK-1069 (1969)
9. F. Voß, S. Cierjacks, these proceedings, contribution C 13
10. C. Allard, private communication
11. J.A. Harvey, Proc. Conf. Pulsed High Intensity Neutron Sources, 1966, USAEC CONF-650217, p.124

12. G.A. Bartholomew, P.R. Tuncliffe, Intense Neutron Generator, 1966, AECL-2600
13. A. Michaudon, Proc. Sem. Intense Neutron Sources, Santa Fe', September 1966, USAEC CONF-660925 , p.789
14. W.W. Havens, Proc. Sem. Intense Neutron Sources, Santa Fe', September 1966, USAEC CONF-660925 , p 565
15. E.R. Rae, Experimental Neutron Resonance Spectroscopy, ed. by J.E. Harvey, Academic Press, New York, 1970, p. 60 ff

TABLE I Specifications of the Karlsruhe Time-of-Flight Spectrometer

Accelerated particles	deuterons
Target	natural uranium
Deuteron energy	50 MeV (maximum)
Neutron production rate in pulse	$7 \times 10^{18}$ neutrons/sec
Pulse duration	1,5 nsec
Repetition rate	20,000 - 200,000 pps (variable)
Length of the flight path	195 m
Energy resolution	35 eV at 300 keV (increasing with energy according to the $E^{3/2}$ law)
Resolution of the spectrometer (best actual value)	0,01 nsec/m
Integrated neutron flux for 10 $\mu$ A target current	$2 \cdot 10^4$ neutrons/cm <sup>2</sup> · sec above $E_n = 250$ keV at 195 m



TABLE II Specifications of Accelerator Based Pulsed Neutron Sources

Accelerator	Particles accelerated	Target	Peak current (mA)	Beam energy (MeV)	Pulse duration (nsec)	Max.Rep.rate (pps)	Neutron product. in pulse (n/sec)	Flight-path length (m)	Best nominal resolution (nsec/m)
Geel Linac	electrons	U	5.000	75	10	1,000	$1 \cdot 10^{18}$	30-400	0,025
			2.500	65	50	1,000	$4 \cdot 10^{17}$		
Geel Linac (improved) <sup>1</sup>	electrons	U	10.000	180	3	1,000	$4 \cdot 10^{18}$	30-400	0,008
			2.000	130	100	880	$7 \cdot 10^{17}$		
Harwell Linac	electrons	U	1.000	45	10	500	-	100	0,1
		U <sup>235</sup> booster	500	42	100	500	$5 \cdot 10^{17}$	5-300	0,5
Oak Ridge Linac	electrons	Ta	15.000	140	2,5-24	1,000	$4 \cdot 10^{18}$	10-200	0,01
			500	140	1000	1,000	$1 \cdot 10^{17}$		
Saclay Linac	electrons	U	3.500	60	20	1,000	$1,5 \cdot 10^{18}$	5-200	0,1
			1.500	65	50	1,000	$7 \cdot 10^{17}$		
Harwell Synchrocycl.	protons	W	3.000	150	4	8,000	$3 \cdot 10^{19}$	8-100	0,04
Karlsruhe SFC	deuterons	U	2.000	50	1,5	200,000	$7 \cdot 10^{18}$	10-195	0,007

<sup>1</sup> Proposed improvement for 4 sections and new gun (C. Allard, 1972)

Figure Captions

- Fig. 1 Scheme of the "deflection bunching" system.
- Top view of the cyclotron chamber showing the position of the deflectors.
  - Schematic drawing illustrating the deflection of ion packets onto the neutron producing target.
- Fig. 2 Voltages applied to the inner deflector system illustrating the principle of beam suppression:
- Elimination of "two out of three" microstructure pulses with a radial deflector.
  - Formation of 4,5  $\mu$ sec ion packets with an additional axial deflector of system I.
- Fig. 3 Typical unmoderated neutron time-of-flight spectrum obtained from bombardment of a natural uranium target with 50 MeV deuterons.
- Fig. 4 Top view of the spectrometer arrangement at the Karlsruhe sector-focussed cyclotron.
- Fig. 5 Total neutron cross section of oxygen from 3 to 7 MeV measured with a resolution of 0.02 ns/m.
- Fig. 6 Differential elastic scattering cross section of calcium between 0.75 - 1.15 MeV determined at  $54^\circ$ ,  $90^\circ$  and  $140^\circ$  to the incident neutron beam with a resolution of 0.05 ns/m.
- Fig. 7 Cross section for the production of the 846 keV  $\gamma$ -line by inelastic neutron scattering in  $^{56}\text{Fe}$  between 0.8-4.5 MeV determined with a resolution of 0.05 ns/m.
- Fig. 8 Useful neutron fluxes available at the detector for several accelerators presently in operation, assuming an effective energy resolution of  $\Delta E/E = 8.8 \cdot 10^{-4}$ . HB = Harwell booster, ORL = Oak Ridge electron linac, HSC = Harwell synchrocyclotron, KSFC = Karlsruhe sector-focussed cyclotron, (comp. ref. 15).

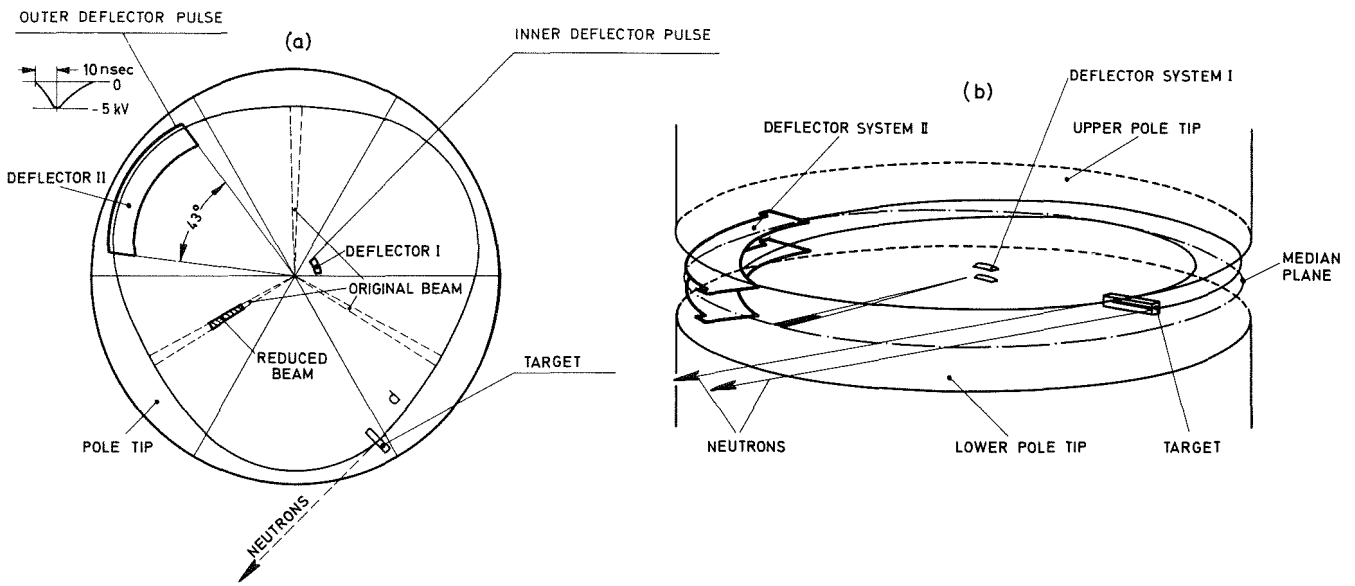


Fig. 1

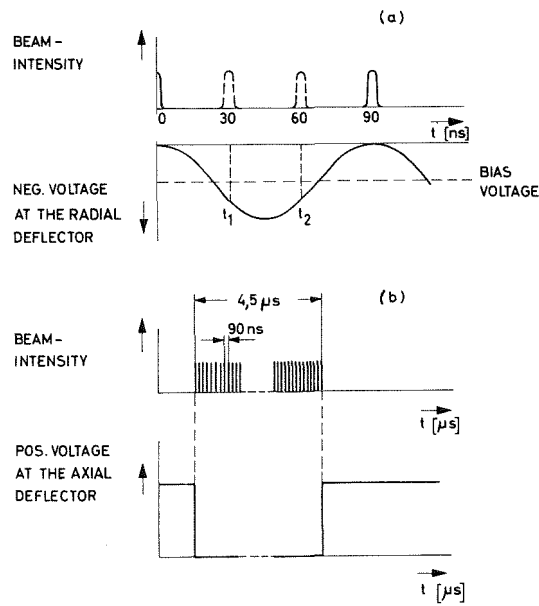


Fig. 2

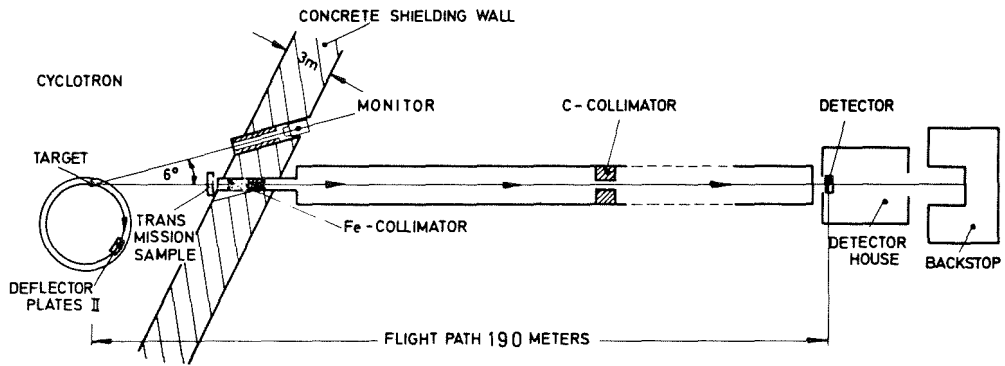


Fig. 3

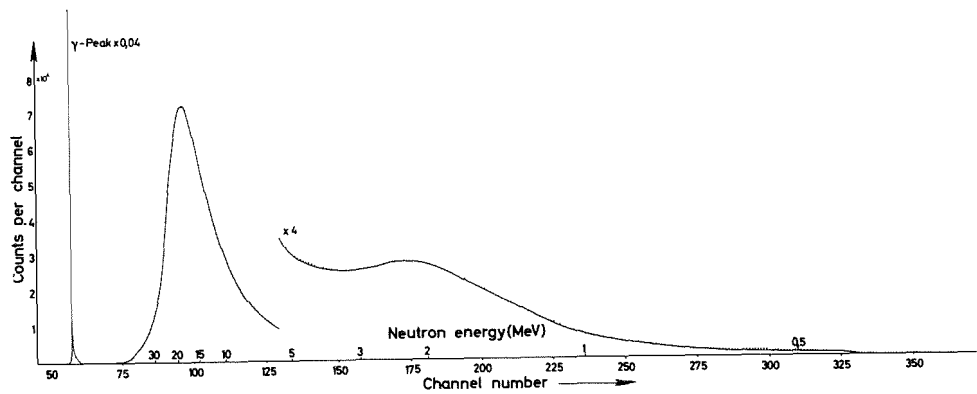


Fig. 4

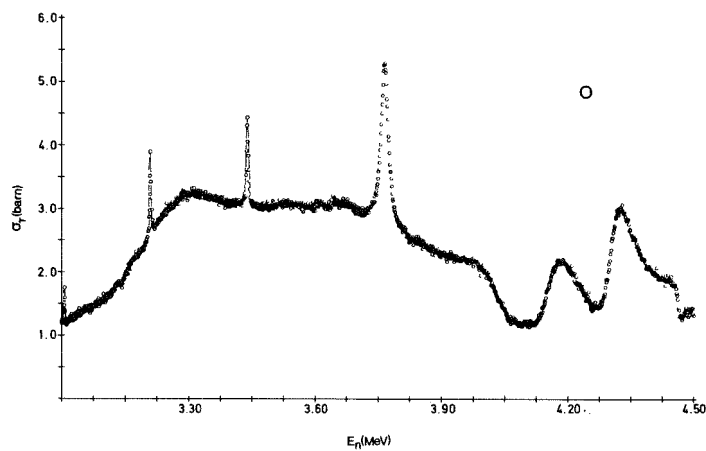
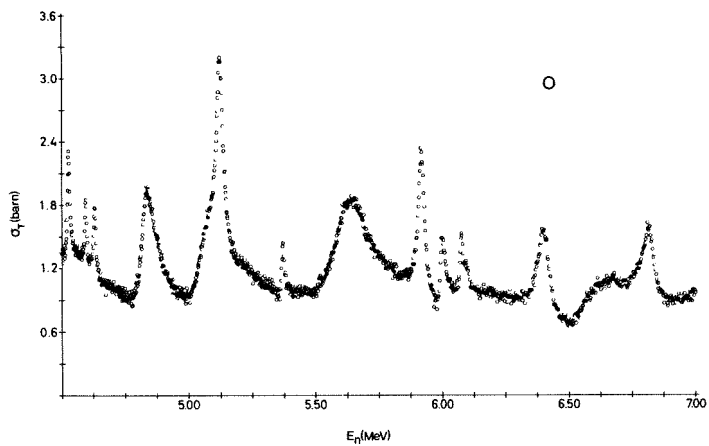


Fig. 5

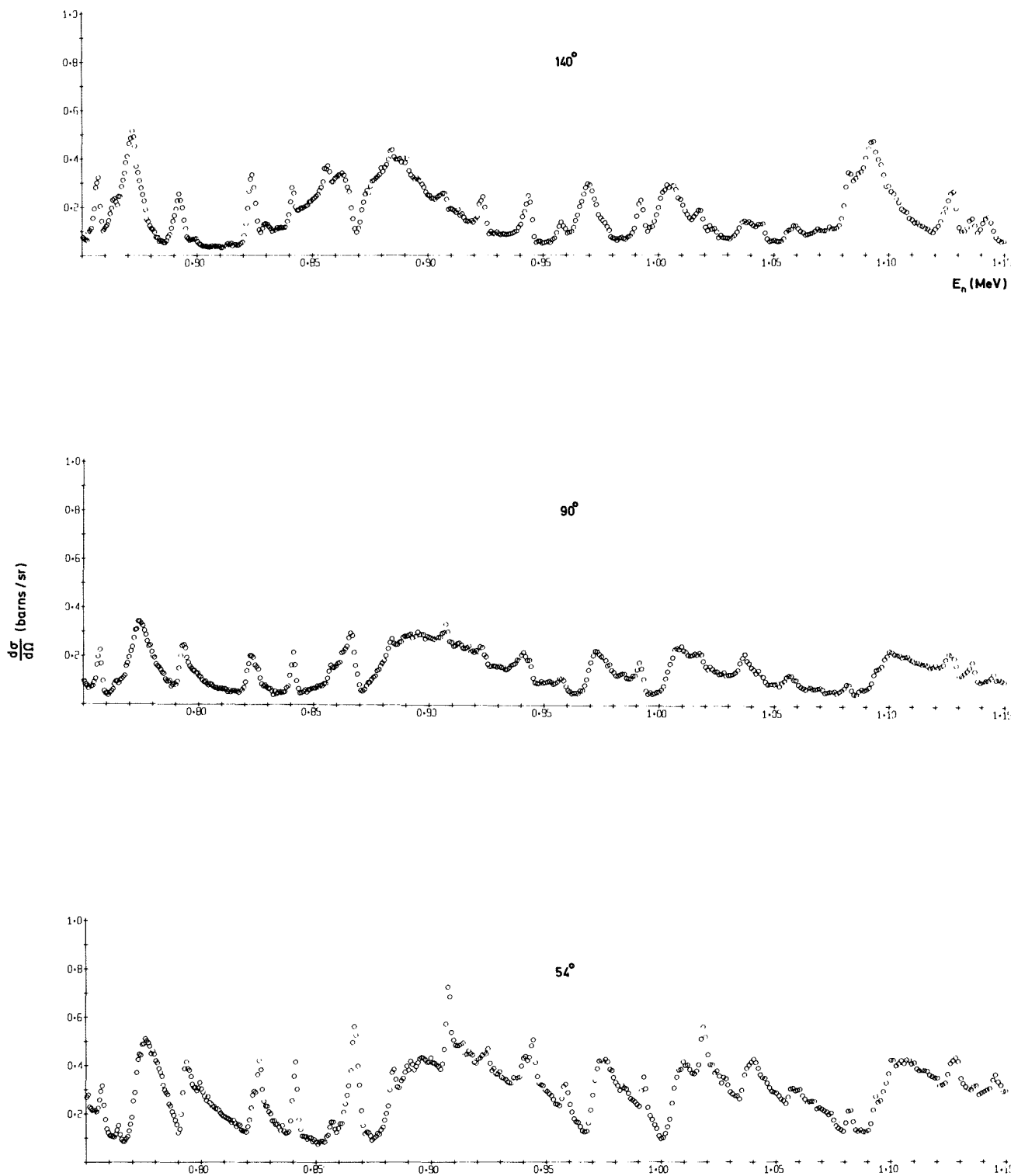


Fig. 6

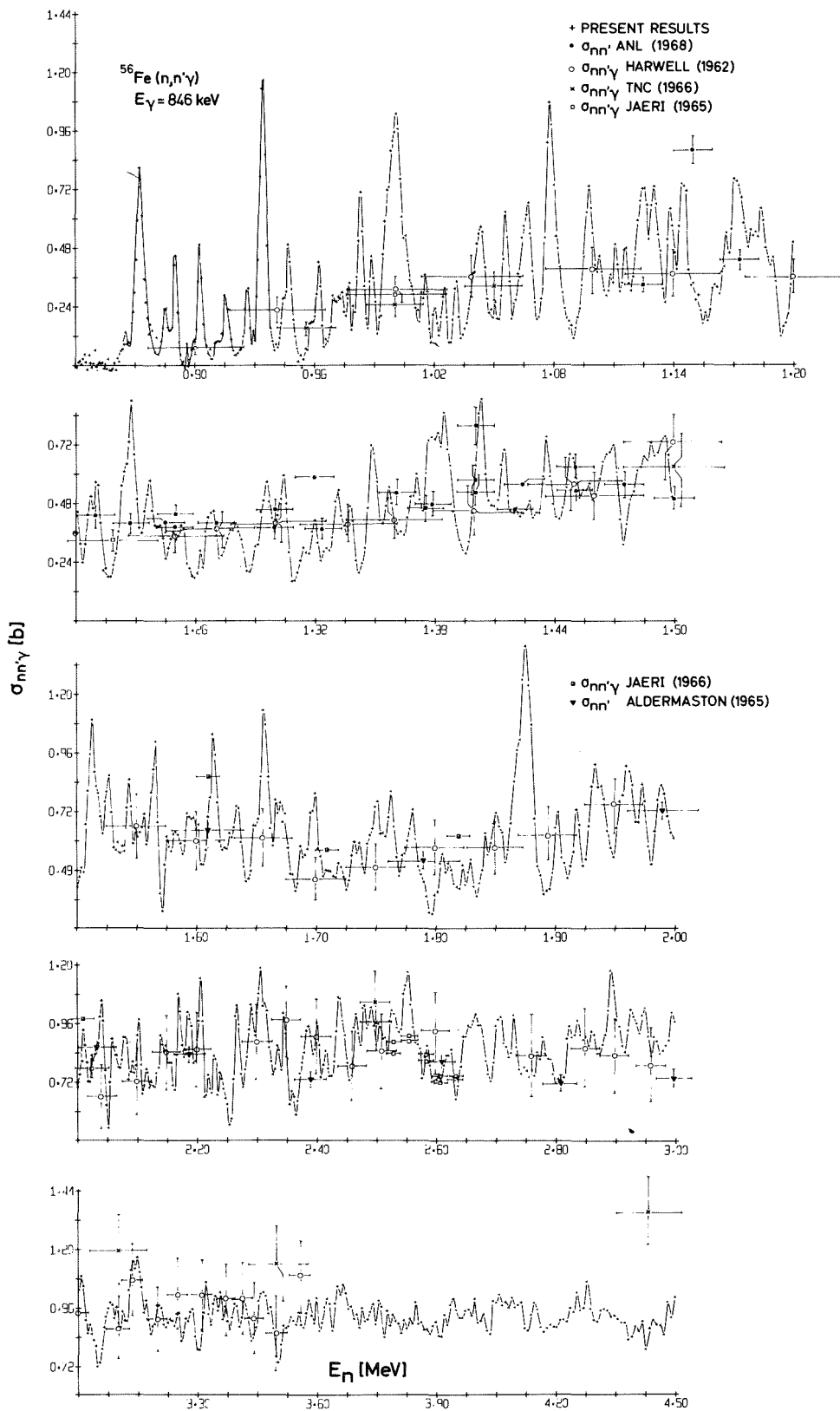


Fig. 7

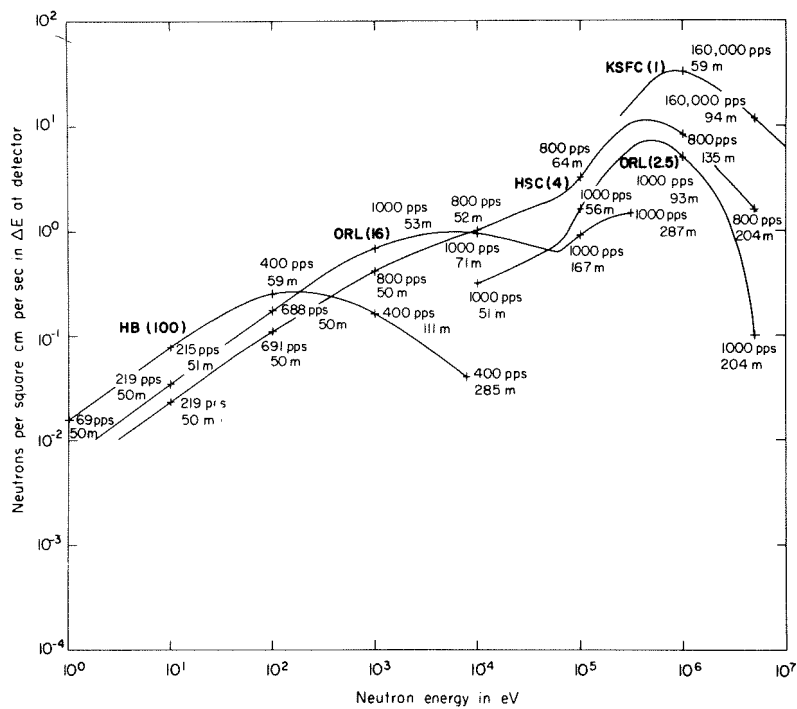


Fig. 8